WILDFIRE-INDUCED FLOODING AND EROSION-POTENTIAL MODELING: EXAMPLES FROM COLORADO, 2012 AND 2013

Steven E. Yochum, Hydrologist, US Forest Service, National Stream & Aquatic Ecology Center, Fort Collins, CO, steveneyochum@fs.fed.us; **John B. Norman, Soil Scientist**, NRCS, Soil Survey Division, Fort Collins, CO, john.norman@co.usda.gov.

prepared for the 5th Federal Interagency Hydraulic Modeling Conference
April 19-23, 2015, Peppermill Hotel, Reno, Nevada, USA

Abstract: Flooding and erosion potential for the High Park, Black Forest and West Fork Complex wildfires, in Colorado, were modeled using the Natural Resources Conservation Service (NRCS) curve number (CN) and Revised Universal Soil Loss Equation (RUSLE) methodologies. The CN technique, implemented within HEC-HMS, estimated direct runoff from rain events for both pre- and post-fire conditions, to develop estimates of increased flood hazard and potential threat to life and property. A spatial version of RUSLE was developed to predict pre- and post-fire sediment yields for each 10x10 meter area for hydrologic flow paths connected to the burn area. The pre- and post-fire CN runoff and RUSLE sediment erosion estimates were summarized at strategically-located pour points within and downstream of the wildfire burn areas. Results were computed at 96 pour points for the High Park Fire (87,000 acres), 52 pour points for the Black Forest wildfire (14,300 acres), and 70 pour points for the West Fork Complex wildfire (109,000 acres). Post-fire conditions were simulated to result in 100-year floods from 10-year rainfall events in the most severely-impacted watersheds and up to 70 to >200 times of sediment expected on an annual basis. The results are most appropriately used in a comparative manner, between catchments.

INTRODUCTION

The 2012 and 2013 Colorado wildfire seasons resulted in 20 substantial fires, including the West Fork Complex, Black Forest, and High Park (Figure 1) wildfires. Wildfires induce substantially increased flooding and erosion potential, with resulting impacts to life and safety, transportation and water supply infrastructure, property, and ecosystems. To address these issues, land managers, planners, and emergency response officials need prompt and spatially-explicit predictions of expected increases in flooding and sedimentation.

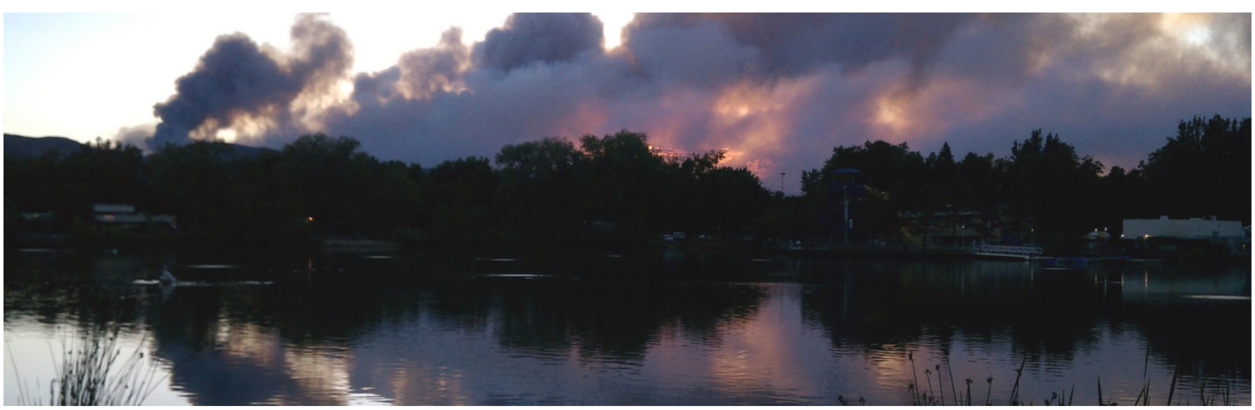

Figure 1 High Park Fire as viewed from Fort Collins, on day 1.

In response to requests from local, state, and federal agency partners, flooding and erosion potential for the High Park, Black Forest and West Fork Complex wildfires were modeled. The NRCS curve number (CN) and Revised Universal Soil Loss Equation (RUSLE) methodologies were implemented. The CN technique estimated direct runoff from rain events for both pre- and post-fire conditions, to develop estimates of increased flood hazard and potential threat to life and property. A spatial version of RUSLE was developed to predict pre- and post-fire sediment yields for each 10x10 meter area for hydrologic flow paths connected to the burn area. The pre- and post-fire CN runoff and RUSLE sediment erosion estimates were summarized to strategically-located pour points within and downstream of the wildfire burn areas. The magnitude of change in sediment yield and runoff were calculated for every pour point, to facilitate interpretation.

An overview of the implemented methods and results are provided, to assist other scientists and engineers with the task of providing officials with estimates of increased flooding and erosion potential after a wildfire. Similar approaches have been implemented by other workers (Livingston et al. 2005; Springer and Hawkins, 2005; Larsen and MacDonald, 2007; Rulli et al. 2013). Other tools are preferred by some practitioners (Canfield et al. 2005, Goodrich et al. 2005); Kinoshita et al. (2014) and Chen et al. (2013) provide comparisons between the results of differing methods. Due to limitations in modeling tools and data availability, and limits in scientific understanding of wildfire hydrology processes, these analysis results are most appropriately used in a relative manner for comparing runoff and sediment liberation potential between catchments. Despite this limitation, the provided methods do produce quantifiable results that are helpful for the informed development of response and restoration priorities, to protect life, property, and infrastructure in the hectic months that follow a wildfire.

METHODS

Wildfires cause hydrologic shifts for a number of years. Substantially increased runoff and sediment production result from the loss of vegetation and soil cover, as well as from hydrophobicity, where the fire-induced vaporization of hydrophobic compounds causes water to collect on the soil surface and run off, instead of infiltrate. The lack of vegetation interception and soil infiltration, from the loss of surface roughness from ground litter and hydrophobicity, can shift the rainfall response from infiltration-dominated processes to surface runoff-dominated processes. For example, watershed impacts due to recent wildfire caused a Swiss catchment to produce 100-year to 200-year runoff discharges from a 10-year rainfall event due to changes in infiltration capacity (Conedera et al. 2003), though scale effects with greater runoff enhancement in smaller catchments and tendencies towards overestimation in larger catchments have been noted (Stoof et al. 2011). Hydrophobicity, which tends to be more prevalent with increased sand content and lower soil water content, has been found to weaken within a few months of a fire but persist for at least 22 months in ponderosa and lodgepole pine forests of the Colorado Front Range (Huffman et al. 2001). Post-fire sediment yield is most dependent on ground cover, with percent ground cover explaining more than 80 percent of the variability in sediment yield (Benavides-Solorio and MacDonald 2001). Soil burn severity is hence fundamental for predicting sediment yield increases.

Predictions of post-fire sediment yield rely on mathematical models such as Revised Universal Soil Loss Equation RUSLE (Renard et al., 1997), Water Erosion Prediction Project WEPP (Elliot, 2004) and GeoWEPP (Renschler, 2003), as well as professional judgment (Robichaud et al., 2000). These methods have varying advantages and disadvantages for estimating the spatial distribution of post-fire soil loss, but all methods can require large amounts of time and energy to estimate soil loss and its associated risks over large spatial extents. With wildfires becoming more pronounced in the wildland-urban interface, rapid watershed management actions to protect sociological concerns, water quality, and ecosystem health are needed. This need for a rapid response to evaluate and manage post fire soil loss has increased the interest in using Geographic Information System (GIS) technology to spatially model post fire sediment yields. This has produced toolsets that use the above models as engines to estimate soil loss rates spatially.

Rainfall-runoff modeling was performed to simulate the expected flood response of the streams draining the wildfire areas. Additionally, predictions of post-fire sediment yield were developed using RUSLE. The implemented methods are presented below. Additional details are provided in the project reports (Yochum 2012; Yochum and Norman 2014).

Runoff Modeling

Runoff modeling was performed using the program HEC-HMS (version 3.5). The NRCS curve number (CN) technique for estimating direct runoff from rain events, combined with the NRCS dimensionless unit hydrograph method, was implemented. As documented in NRCS (2004b), the NRCS method for estimating direct runoff from individual storm rainfall events is of the following form:

$$Q = \frac{\left(P - I_a\right)^2}{\left(P - I_a\right) + S} \text{ if } P > I_a \quad (1)$$

$$Q = 0 \qquad \text{if } P \le I_a \quad (2)$$

where Q is the depth of runoff (inches), P is the depth of rainfall (inches), I_a is the initial abstraction (inches), and S is the maximum potential retention (inches). The equation derivation is not physically based but does respect conservation of mass (NRCS 2004b).

The Curve Number (CN) is defined as:

$$CN = \frac{1000}{10 + S} \quad (3)$$

The initial abstraction was initially described and has traditionally been used as:

$$I_a = 0.2S \quad (4)$$

To reflect the decreased storage of a fire impacted soil surface (due to a reduction of depression storage from the elimination of soil litter), the initial abstraction was assumed to be 0.1S for post-wildfire conditions in catchments that were substantially burned (>50% moderate + severe soil burn severity). Catchments that were not substantially burned were modeled with the standard I_a of 0.2S. The impact of the I_a adjustment on CNs was ignored; for the high CN (post-wildfire) conditions, smaller shifts in CN due to changes in I_a can be expected (Woodward et al. 2003).

The CN is a simple catchment-scale method that gives simplified results at a stream outlet, with more accurate results expected for larger, higher-intensity rain events. The method is documented is in the NRCS National Engineering Handbook, Part 630, Hydrology, Chapters 9 and 10 (NRCS 2004a, NRCS 2004b), in Rallison (1980), as well as in numerous other publications. However, little quantitative information has been published of the database on which it was developed (Maidment 1992). In general, the method was developed for rural watersheds in various parts of the United States, within 24 states; was developed for single storms, not continuous or partial storm simulation; and was not intended to recreate a specific response from an actual storm (Rallison, 1980).

An overview of the general weaknesses of the CN method is provided in Hawkins (2014). Specifically in regard to rainfall-runoff modeling for wildfire areas, the reliability of the CN method for predicting peak flow from forested, mountainous watersheds is debatable. Forested watersheds in unburned conditions may be dominated by saturation-excess overland flow, where runoff is produced from relatively small and variable portions of a catchment when rainfall depths exceed the soil capacity to retain water. Newly burned catchments, on the other hand, may likely be dominated by infiltration-excess (Hortonian) overland flow, where surface runoff is generated when rainfall intensity is greater than soil infiltration capacity, and flow runs down the hillslope surface. Evidence of this surface runoff is provided by such features as surface rilling on freshly-burned hillslopes. Rainfall-runoff modeling performed in the San Dimas Experimental Forest (Chen et al. 2013) found that pre-fire runoff predictions were more accurate using the CN method, while KINEROS2 performed better for post-fire conditions. These results suggest fundamental shifts in runoff mechanisms between pre- and post-fire conditions, complicating modeling strategies. CN values are not well known for burned conditions, which is a primary source of potential error. Additionally, spatial rainfall variability due to orographic forcing can lead to additional modeling uncertainty, for the CN method as well as other rainfall-runoff modeling tools.

Despite the method's shortcomings, due to its relative simplicity, achievable data requirements on large scales, and the relatively-short timeframe needed to develop a model, as well as at least qualitatively-reasonable results when compared to actual post-fire runoff events, the CN method is a preferred tool for predicting the flow responses of wildfire areas. The best use of the modeling results is through comparison of different catchments flood response to identical rainfall events, for the prioritization of areas of concern. The use of peak flow ratios (i.e. post-fire peak flow/pre-fire peak flow) can be the most effective tool for comparisons.

CN

Curve numbers are values less than 100, with higher values corresponding to catchments with lower infiltration rates and higher runoff potential. In general, CN assignments are typically made using guidance provided in NRCS (2004a). CNs were assigned throughout the modeled catchments according to hydrologic soil group, vegetative type, and soil burn severity (Table 1). Soil burn severity is a dominant factor in CN assignments in burned areas. The average catchment CN was computed using an aerial averaging methodology. Catchment size was limited to areas that have similar runoff characteristics, and, where possible, to 2000 acres. As catchment size increased, CNs were computed for adjacent and serial catchments and flows were modeled, routed downstream, and combined with lower catchments to predict flow at downstream points of interest (Figure 2).

Table 1 CN assignments.

Cover Description	**A** HSG				**B** HSG				**C** HSG				**D** HSG			
	Unburned	Low	Moderate	High	Unburned	Low	Moderate	High	Unburned	Low	Moderate	High	Unburned	Low	Moderate	High
Herbaceous, Pasture, Alpine Meadow, Park	49	55	67	77	61	68	80	86	74	81	88	89	82	86	92	95
Oak-aspen—mountain brush mixture of oak brush, aspen, mountain mahogany, bitter brush, maple, and other brush	45	52	65	77	48	55	65	86	57	70	80	89	63	70	80	92
Ponderosa pine-juniper (grass understory)	49	57	65	77	58	65	75	86	73	78	83	89	80	85	90	92
Sagebrush (grass understory)	46	54	65	77	51	60	75	86	63	70	80	89	70	75	85	92
Lodgepole Pine Forest	49	57	65	77	60	65	70	86	73	78	83	89	79	83	87	92
Bare soil	77	77	77	77	86	86	86	86	91	91	91	91	94	94	94	94
Wetland	98	98	98	98	98	98	98	98	98	98	98	98	98	98	98	98

Hydrologic soil group (HSG) classifications were selected using soils data published in the NRCS SSURGO (Soil Survey Geographic) database. Using this method, soil are classified as being either A, B, C, or D type, where A allows the most infiltration and least runoff and D allows the least infiltration and greatest runoff. Vegetation type, from SWReGAP (Southwest Regional Gap Analysis Project) land cover mapping, was included in the CN assignments used for the modeling. Soil burn severity is the principle driver for increasing flow in runoff predictions. For these wildfires, soil burn severity was measured using the BARC process from satellite imagery.

A fair ground cover condition was generally assumed for the unburned values (Table 1) abstracted from NRCS (2004a), though a good ground condition was assumed for herbaceous/grassland. The CN values for burned conditions were primarily compiled from various grey literature and unpublished sources; they are approximate. Research is needed to better define these values.

Rainfall, Lag Time, Flow Routing, and Sediment Bulking

Rainfall depths used in the modeling were extracted from NOAA Atlas 14, Vol 8 (Perica et al. 2013), for the West Fork and Black Forest fire areas, and from NOAA Atlas 2, Volume 3 (Miller et al. 1973) for the High Park fire area. Six-hour rainfall durations and NRCS Type II rainfall distributions were assumed for the West Fork Complex Wildfire while 1-hour durations and TR-60 distributions were implemented for the Black Forest and High Park Wildfires. Areal reduction factors were applied as detailed in Miller et al. 1973. Where applied, these area reductions were implemented in all catchments; flow may be underpredicted in the smaller, upper catchments of such drainages.

Lag time (L), which is required to generate a hydrograph using the NRCS unit hydrograph methodology, was computed using the watershed lag method (NRCS 2010). The lag equation is:

$$L = \frac{l^{0.8}\left(S+1\right)^{0.7}}{1900Y^{0.5}} \tag{5}$$

, where l is the flow length (ft), Y is the average watershed land slope (%), and S is the maximum potential retention (in),

$$S = {1000}/{cn'} - 10 \tag{6}$$

, where *cn'* is the retardance factor and is approximately equal to the CN. This method allows the rapid computation of differing lag times for pre- and post-fire conditions, reflecting the physical mechanism of more rapid flow response during post-fire conditions.

A Muskingum-Cunge procedure was used to route flow from upper catchments to the stream outlets. This 1-dimensional method allows for flow attenuation in the computations but does not provide a numerical solution of the full unsteady flow routing equations, as provided in such computational models as HEC-RAS. In each reach, flow routing was estimated using a single simplified cross section, channel slope, and Manning's *n* roughness estimates. Manning's *n* was selected using a visual estimation procedure, with a quality control step to assure that to maintain subcritical or approximately critical velocity was maintained, reflecting an assumption that existing or new channel bedform development prevents reach-average supercritical flow.

A simple multiplication factor was applied to the post-fire flood predictions to account for sediment bulking in the debris flows. For burned catchments, this multiplication factor was assumed to be 1.25 if the severe plus moderate soil burn severity aerial extent was greater than 50%, and 1.1 for catchments with between 15 and 50% soil burn severity.

Sediment Modeling

The RUSLE model was chosen to estimate pre- and post-fire sediment erosion rates. The RUSLE models (pre and post fire) are based on a spatial version of RUSLE outlined in Theobald et al. (2010) and Litschert et al. (2014). The ATREW methods entail calculating RUSLE (Equation 7) the standard way using widely available fine resolution spatial datasets to approximate the 6 RUSLE factors. The ATREW report provides guidance on parameterizing the RUSLE *C* and *P* factors based on commonly used landcover datasets (e.g., USGS National Landcover Dataset and USFS Existing Vegetation Dataset), as well as equations that scale GIS based terrain analysis for the *L* and *S* factors.

The advantages of this approach are (1) simple model parameterization using nationwide spatial datasets; (2) production of a sedimentation rate raster (each raster cell has a sedimentation rate); and (3), evaluate the resulting sediment yield rasters spatially to help prioritize soil treatment zones and emergency resource allocation. The RUSLE equation is:

$$A = R \cdot K \cdot L \cdot S \cdot C \cdot P \quad (7)$$

where A is the average annual unit-area (tons per hectare per year), R is the rain erosivity factor (Mj mm/(ha h yr)), K is the soil erosivity factor, L is the slope length factor (m), S is the slope steepness factor, C is the cover management factor (>= 0), and P representing the management factor (>= 0). The sediment modeling entailed 4 general steps: (1) collection of geospatial dataset for the greater burn area (Table 2); (2) development of spatial RUSLE factors for pre and post fire conditions; (3) calculate RUSLE for pre- and post-fire scenarios (ArcGIS Raster Calculator); and (4) attribute computation points and values at risk with pre- and post-fire sedimentation rates. Pre- and post-fire sedimentation rate estimates were executed within a GIS using terrain analysis tools to calculate slope length (L) and steepness (S) factors with simple map algebra statements used to compute rainfall erosivity (R), soil erodibility (K) and cover management (C) factors from ancillary spatial datasets. The soil/cover management (P) factor was not incorporated in the analysis due to a lack of spatial information on management activity in the burn area. For each of the five RUSLE factors used, a 10-meter resolution raster dataset was generated. The five RUSLE factor rasters where multiplied together to calculate the local (cell level) sedimentation rate. The local sedimentation rate values were accumulated downslope via a flow direction raster (Yochum and Norman 2014) and averaged by the contributing area above each raster cell. This results in the final sedimentation rate raster with values representing the average cumulative sedimentation rate in tons per year over 30 years for each scenario.

The rain erosivity (*R*) factor raster was generated by rasterizing the EPA EMAP HUC 8 polygon shapefile to a raster containing *R* factor values. The *R* factor raster was held constant between the pre- and post-fire scenarios due to a lack of information about change in rain erosivity values and the EPA EMAP values are based on 30 year averages. The HUC 8 *R* factor raster was masked out to match the cell size and processing extent.

Table 2 Spatial datasets sources used for the six RUSLE factors.

Factor	Source
R	U.S. Enviromental Protection Agency EMAP-West RUSLE Factors
K	USDA NRCS Web Soil Survey SSURGO spatial and tabular data
L & S	USGS National Elevation Dataset
C	USGS National Gap Analysis Program 30 meter landcover
P	Parameter not used in analysis due to lack of good spatial data

The development of soil erodibility (*K*) factor raster entailed summarizing KFFACT (SSURGO table attribute) to NRCS SSURGO map units and then rasterizing the map units in the same manner as the *R* factor. KFFACT (property of a soil horizon) was summarized to map unit delineations by calculating a depth/area weighted average based on horizon depths up to 15 centimeters and the component percent within a map unit. This was accomplished through queries developed in the SSURGO database downloaded from the USDA Geospatial Data Gateway website. The *K* factor raster was held constant for both scenarios even though burn severity alters soil erodibility. Altering soil erodibility based on burn severity between scenarios could be incorporated in future models but would require additional research.

The *L* and *S* factor were calculated jointly (*LS*) using basic terrain analysis methods outlined in Theobald et al. (2010) using a 10 meter elevation model. These methods include calculating a percent slope, aspect (radians), and accumulated upslope length. The accumulated upslope length process entailed accumulating number of contributing raster cells to a given cell based on the overland flow paths from the flow direction raster. The resulting slope, aspect and upslope length rasters were transformed using equations developed by Winchell et al. (2008, Equation 8) and Nearing (1997, Equation 10). These equations scale the values derived from the above terrain analysis to better fit within the frame work of the RUSLE equation and ensure that the units are correct. The slope length scaling equation is

$$LS_{i,j} = S_{i,j} * \frac{(A_{ij}+D^2)^{m+1} - A_{ij}{}^{m+1}}{X_{i,j}^{m+2} \cdot D^{m+2} \cdot 22.13^m} \quad (8)$$

, where LS_{ij} is the transformed slope length, *D* is the cell size of the analysis (10 meters), *X* aspect transformation (Equation 9), *m* slope transformation (Equation 10) and $S_{i,j}$ is the slope transformation function derived by equation 11. Aspect transformation were computed through:

$$X_{i,j} = \sin \alpha_{i,j} + \cos \alpha_{i,j} \quad (9)$$

, where $X_{i,j}$ is the transformed aspect values for raster cell *I* and *alpha* is aspect (radians clockwise from north) for raster cell *I*. Radians was used instead of degrees from north to prevent negative values from occurring when calculating COS of aspect in ESRI ArcGIS. The slope transformation is

$$\beta = \frac{\frac{\sin\theta_{i,j}}{0.0896}}{3(\sin\theta_{i,j}^{0.8}+0.56)} \tag{10}$$

, where *theta* is percent slope and the *m* coefficient is calculated by taking the ratio between *beta* and one plus *beta* ($\beta / 1 + \beta$).

The slope length ($LS_{i,j}$) factor raster was developed using the Nearing (1997) equation (Equation 8) in conjunction with equations 9, 10 and 11 to account for aspect and slope dynamics to better scale large flow path values (accumulated slope length). This is necessary because the accumulated flow path raster (A_{ij}) can have very large values which inflate sedimentation estimates. The *S* factor raster was developed by transforming percent slope using equation 11. Equation 11 scales slope values to reduce inflated soil loss values especially for slopes greater than 50%. As with the *R* and *K* factors the *L* and *S* factors were held constant between the pre and post fire models. The *S* factor transformation is computed as

$$S_{i,j} = 1.5 + \frac{17}{1+e^{(2.3-6.1*\sin\beta)}} \tag{11}$$

, where *beta* is the mean slope angle (Equation 10).

The *C* factor parameterization for the pre- and post- fire scenarios was developed using various source tables from different documents related to RUSLE. The pre-fire scenario parameterization involved developing a lookup table that assigns the existing landcover types (Southwest ReGAP) within the greater burn area their associated *C* factors (Yochum and Norman 2014). Table 3 in this project report was compiled by Theobald et al. (2010) for the ATERW report and provides a broad spectrum of landcovers found in most landcover datasets and can be modified based on local knowledge. The post-fire *C* factor parameterization entailed modifying the pre- burn *C* factor raster based on burn severity classes derived from the Burned Area Reflectance Classification (BARC) image. This process consisted of assigning the BARC burn severity classes *C* factor values (low burn = 1.03, moderate burn = 2.25 and high burn 3.75) (Larsen et al., 2007) that were then used to modify the pre-fire *C* factors by summing the two rasters together. Larsen et al. (2007) estimated that high burn severity area *C* factors changed by four hundred percent but didn't estimate moderate and low burn severity changes. *C* factors changes were selected using professional judgment.

The final sedimentation rate models for the pre- and post-fire scenarios were generated by first multiplying the 5 factors, accumulating the multiplied values downslope via the flow direction raster, and calculating an area weighted sedimentation rate. The area weighted sedimentation rate is calculated by dividing the accumulated sedimentation rate by the total accumulated drainage area (Yochum and Norman 2014). This aspect approximates the transportation of sediment from areas where sediment originates (steep slopes or burned areas) to areas that dampen sediment transport due to decreases in slope, unburned areas or flow distance. This assumes that sediment yields decreases from source areas downslope as slope decreases and distance increases.

RESULTS AND DISCUSSION

The results from the these three sets of models provided useful estimates of post-fire flooding and sedimentation rates that officials have used to prioritize management activities to reduce risk to life, property and infrastructure. Due to modeling limitations, the results are most appropriately used in a relative manner, comparing runoff and sediment liberation potential between catchments.

The 70 pour points for West Fork Complex wildfire (109,000 acres) indicate that severely burned catchments would experience a 50- or 100-year flood from a 10-year rainfall event and that 25-year rainfall events would produce more than 12 times the peak flow at some locations (Figure 2). Example maps produced for the project report are illustrated (Figures 3 and 4). The sediment modeling predicts that, on average, all catchments will experience 130 times more sediment, with one burn area (Papoose wildfire) accounting for 65% of the total sediment predicted to be delivered to the Upper Rio Grande river from the two fires.

Results at ninety six pour points were computed for the High Park wildfire (87,000 acres). Post-fire conditions were commonly predicted to induce 50- or 100-year floods from 10-year rainfall events across the High Park burn area, with the 25-year rainfall event expected to yield up to up to 10 times the pre-fire peak flow. Additionally, sediment yields were predicted to be 73 times

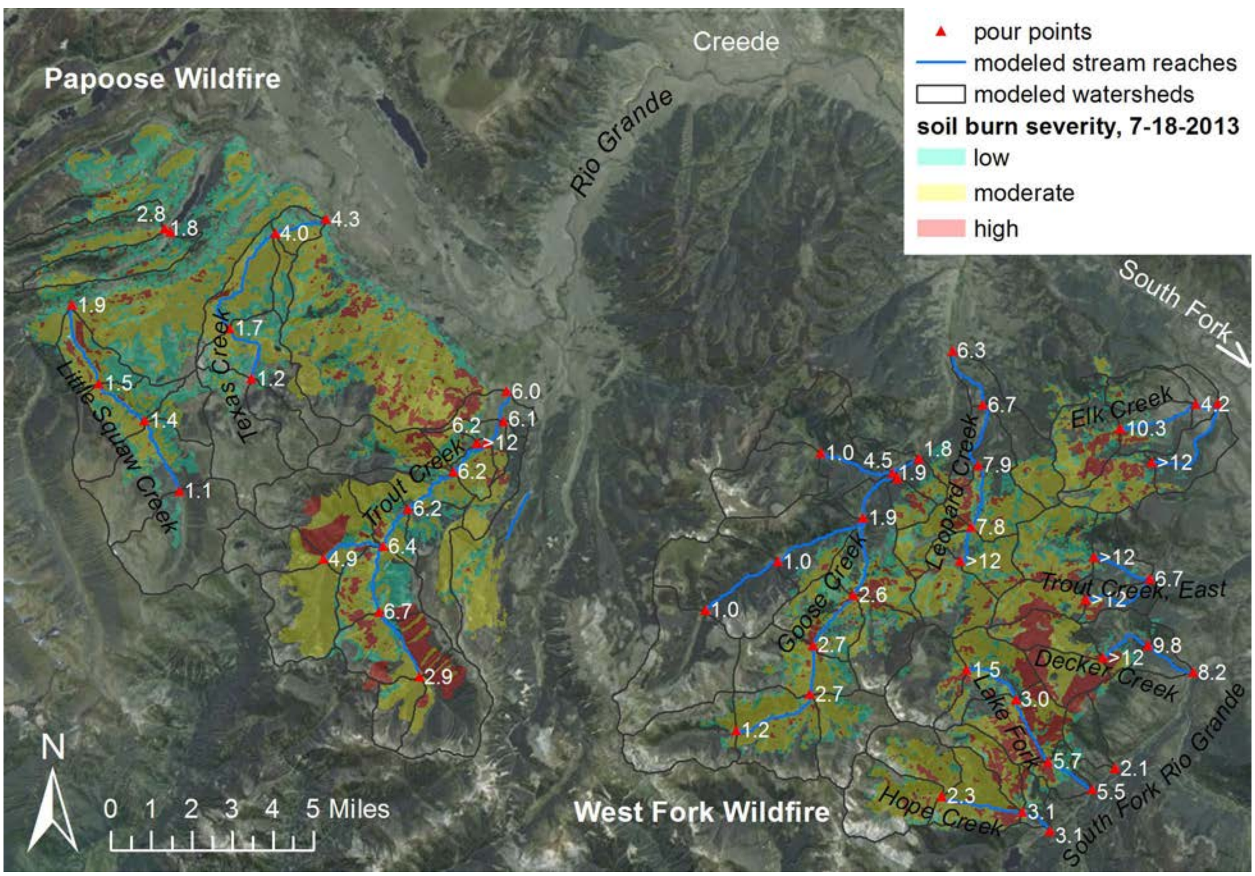

Figure 2 West Fork Complex wildfire peak flow magnification ratios (25-year rain event).

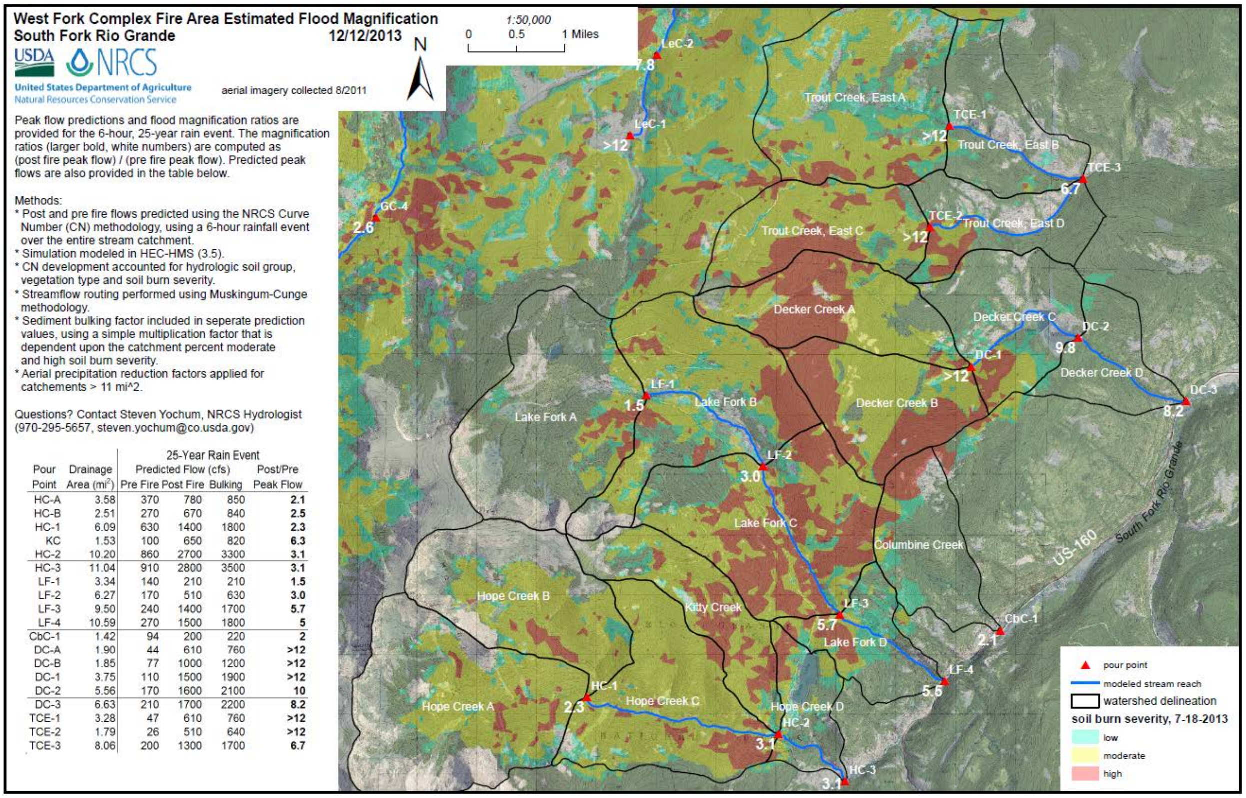

Pour Point	Drainage Area (mi^2)	25-Year Rain Event Predicted Flow (cfs) Pre Fire	Post Fire	Bulking	Post/Pre Peak Flow
HC-A	3.58	370	780	850	**2.1**
HC-B	2.51	270	670	840	**2.5**
HC-1	6.09	630	1400	1800	**2.3**
KC	1.53	100	650	820	**6.3**
HC-2	10.20	860	2700	3300	**3.1**
HC-3	11.04	910	2800	3500	**3.1**
LF-1	3.34	140	210	210	**1.5**
LF-2	6.27	170	510	630	**3.0**
LF-3	9.50	240	1400	1700	**5.7**
LF-4	10.59	270	1500	1800	**5**
CbC-1	1.42	94	200	220	**2**
DC-A	1.90	44	610	760	**>12**
DC-B	1.85	77	1000	1200	**>12**
DC-1	3.75	110	1500	1900	**>12**
DC-2	5.56	170	1600	2100	**10**
DC-3	6.63	210	1700	2200	**8.2**
TCE-1	3.28	47	610	760	**>12**
TCE-2	1.79	26	510	640	**>12**
TCE-3	8.06	200	1300	1700	**6.7**

Figure 3 Example map providing pre- and post-fire flood predictions for the S. F. Rio Grande.

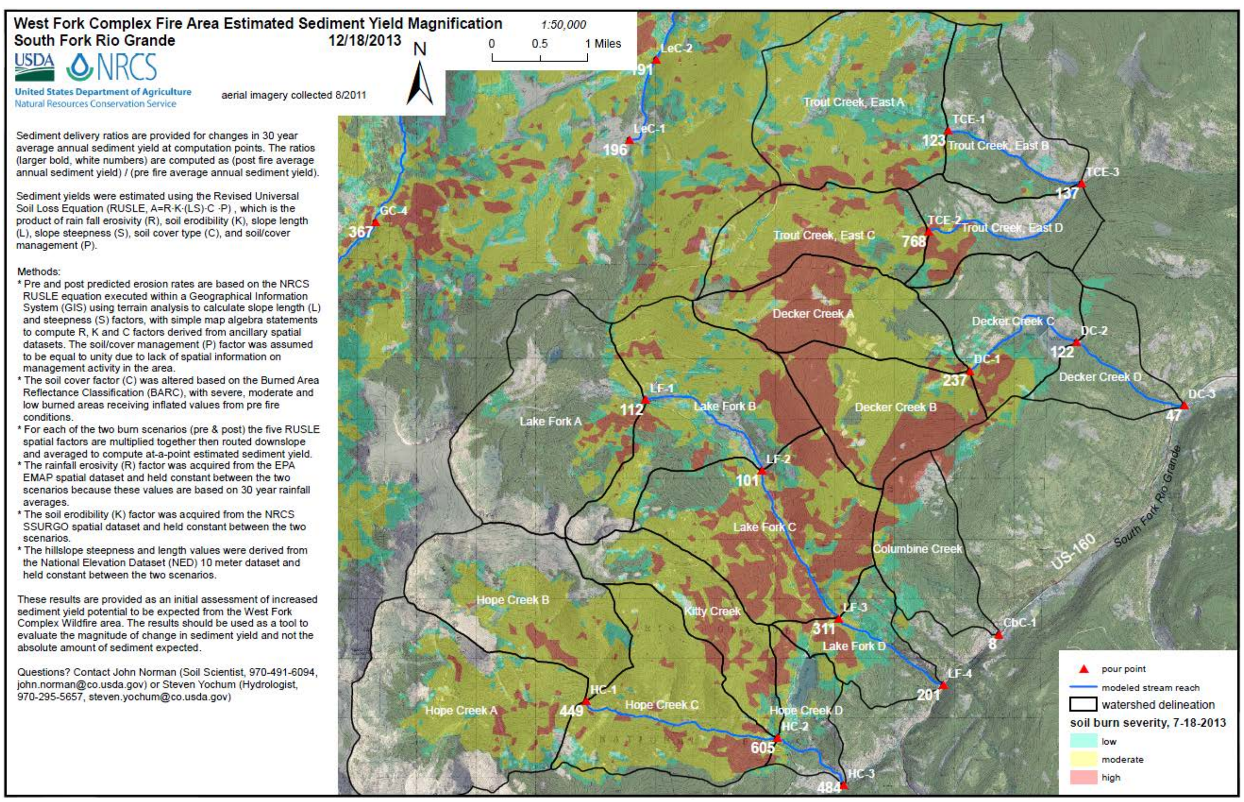

Figure 4 Example map providing pre- and post-fire erosion predictions for the S. F. Rio Grande.

greater than pre-fire conditions, with five catchments of the South Fork of the Cache La Poudre River having sediment magnification rates greater than 200.

Results at the 52 pour points for the Black Forest wildfire (14,300 acres) indicated that values at risk would experience a 100- or 200-year flood event from a 10-year rainfall event, with up to 15 times the pre-fire peak flow expected for the 25-year rainfall event. Sediment yield estimates predict sediment rates 75 times greater than pre-fire conditions with 15 values at risk having sediment magnification rates greater than 200.

CONCLUSIONS

Flow and sediment modeling was performed for the High Park (2012), Black Forest (2013) and West Fork Complex (2013) Wildfires. The results from the these three sets of models have provided useful comparative estimates of post-fire flooding and sedimentation rates (with respect to pre-fire conditions) that officials have used to prioritize management activities to reduce risk to life, property and infrastructure.

Substantial automation of the relatively-simple computational tools used to develop these estimates is possible; with support for the development or refinement of automation tools, results at the spatial scale presented in this report are likely feasible within the relatively-short Burn Area Emergency Response (BAER) process timeline.

ACKNOWLEDGEMENTS

Numerous individuals have contributed fieldwork, review, and other support for the modeling presented in this report. These individuals include David Levinson, Kari Sever, Sam Streeter, John Andrews, Claudia Hoeft, John Segars, Dustin Jager, Randy McKinley, Dan Moore, Jonas Feinstein, Rodney Clark, and Beau Temple. Their assistance has been highly appreciated.

REFERENCES

Benavides-Solorio, J., and MacDonald, L.H. (2001). “Post-Fire Runoff and Erosion from Simulated Rainfall on Small Plots, Colorado Front Range,” Hydrological Processes 15, 2931-2952.

Canfield, H.E., Goodrich, D.C., and Burns, I.S. (2005). “Selection of Parameters Values to Model Post-Fire Runoff and Sediment Transport at the Watershed Scale in Southwestern Forests,” Managing Watersheds for Human and Natural Impacts: pp. 1-12, doi:10.1061/40763(178)48.

Chen, L., Berli, M., and Karletta, C. (2013). “Examining modeling approaches for the rainfall-runoff process 18 in wildfire-affected watersheds: using San Dimas Experimental Forest.” Journal of the American Water Resources Association 1-16, doi:10.1111/jawr.12043.

Conedera, M., Peter, L., Marxer, P., Forster, F., and Rickenmann, D., R, L. (2003). “Consequences of Forest Fires on the Hydrogeological Response of Mountain Catchments: A Case Study of the Riale Buffaga, Ticino, Switzerland” Earth Surface Processes and Landforms 28, 117-129.

Elliot, W.J. (2004). “WEPP Internet interfaces for forest erosion prediction,” Journal of the American Water Resources Association, 40, 299-309.

Goodrich, D.C., Canfield, H.E., Burns, I.S., Semmens, D.J., Miller, S.N., Hernandez, M., Levick, L.R., Guertin, D.P., Kepner, W.G. (2005). “Rapid post-fire hydrologic assessment using the AGWA GIS-based hydrologic modeling tool,” Managing Watersheds for Human and Natural Impacts: pp. 1-12, doi:10.1061/40763(178)44.

Hawkins, R.H. (2014). “Curve Number Method: Time to Think Anew?” ASCE Journal of Hydrologic Engineering 19, 1059-1059, doi:10.1061/(ASCE)HE.1943-5584.0000954.

Huffman, E.L., MacDonald, and L.H., Stednick, J.D. (2001). "Strength and Persistence of Fire-Induced Soil Hydrophobicity Under Ponderosa and Lodgepole Pine, Colorado Front Range" Hydrological Processes 15, 2877-2892.

Kinoshita, A.M., Hogue, T.S., and Napper, C. (2014). "Evaluating pre- and post-fire peak discharge predictions across western U.S. watersheds," J. of the Am. Water Resources Association, 1-18, doi:10.1111/jawr.12226.

Larsen, I. J., and MacDonald, L.H. (2007). "Predicting postfire sediment yields at the hillslope scale: Testing RUSLE and Disturbed WEPP," Water Resources Research, 43 W11412, doi:10.1029/2006WR005560.

Litschert, S.E., Theobald, D.M., and Brown, T.C. (2014). "Effects of climate change and wildfire on soil loss in Southern Rockies Ecoregion." Catena 118, 206-219.

Livingston, R.K., Earles, T.A., and Wright, K.R. (2005). "Los Alamos Post-Fire Watershed Recovery: A Curve-Number-Based Evaluation," Managing Watersheds for Human and Natural Impacts: pp. 1-11. doi:10.1061/40763(178)41.

Maidment, D.R. (1992). Handbook of Hydrology. McGraw-Hill, Inc.

Miller, J.F., Frederick, R.H., and Tracey, R.J. (1973). *"Precipitation-Frequency Atlas of the Western United States."* U.S. Department of Commerce, National Oceanic and Atmospheric Administration, National Weather Service, NOAA Atlas 2, Vol 3, Silver Spring, Maryland.

Nearing, Ma., (1997). "A single continuous function for slope steepness influence on soil loss," Soil Science Society of America Journal, 61 (3), 917-919.

NRCS (2004a). "Hydrologic Soil Cover Complexes," USDA Natural Resources Conservation Service, National Engineering Manual, Chapter 9, 210-VI-NEH, July.

NRCS (2004b). "Estimation of Direct Runoff from Storm Rainfall," USDA Natural Resources Conservation Service, National Engineering Manual, Chapter 10, 210-VI-NEH.

Perica, S., Martin, D., Pavlovic, S., Roy, I., St. Laurent, M., Trypaluk, C., Unruh, D., Yekta, M., Bonnin, G. 2013 *NOAA Atlas 14 Volume 8 Version 2, Precipitation-Frequency Atlas of the United States, Midwestern States.* NOAA, National Weather Service, Silver Spring, MD.

Rallison, R.E. (1980). "Origin and Evolution of the SCS Runoff Equation," Proceedings of the Symposium on Watershed Management; American Society of Civil Engineers, Boise, ID.

Renard, K. G., G. R. Foster, G. A. Weesies, D. K. McCool, and D. C. Yoder. (1997). "Predicting soil erosion by water: A guide to conservation planning with the revised universal soil loss equation (RUSLE)," Agricultural Handbook 703, 404 pp., U.S. Department of Agriculture, Washington, D. C.

Renschler, C. S. (2003). "Designing geo-spatial interfaces to scale process models: The GeoWepp approach," Hydrological Processes, 17, 1005-1017.

Rodichaud, P.R. 2000. Fire effects on infiltration rates after prescribed fire in northern Rocky Mountain forests, USA, J. Hydrol., 231-232, 220-229.

Rulli, M.C., Offeddu, L., and Santini, M. (2013). "Modeling postfire water erosion mitigation strategies," Hydrology and Earth System Sciences, 17, 2323-2337.

Spinger, E.P., and Hawkins, R.H. (2005). "Curve Number and Peakflow Responses Following the Cerro Grande Fire on a Small Watershed." Managing Watersheds for Human and Natural Impacts: pp. 1-12, doi:10.1061/40763(178)40.

Stoof, C.R., Vervoort, R.W., Iwema, J., van den Elsen, J., Ferreira, A.J.D., and Ritsema, C.J. (2011). "Hydrological Response of a Small Catchment Burned by an Experimental Fire," Hydrology and Earth System Sciences Discussions 8, 4053-4098.

Theobald, D.M., D.M. Merritt, and J.B. Norman, III. (2010). "Assessment of Threats to Riparian Ecosystems in the Western U.S. A report presented to The Western Environmental Threats Assessment Center, Priveville, OR by the U.S.D.A.," Stream Systems Technology Center and Colorado State University, Fort Collins, 61p.

Winchell, M.F., S.H. Jackson, A.M. Wadley and R. Srinivasan. (2008). "Extension and validation of a geographic information system-based method for calculating the Revised Universal Soil Loss Equation length-slope factor for erosion risk assessments in large watersheds," Journal of Soil and Water Conservation 63(3): 105-111.

Woodward, D., Hawkins, R., Jiang, R., Hjelmfelt, Jr., A., Van Mullem, J., and Quan, Q. (2003). "Runoff Curve Number Method: Examination of the Initial Abstraction Ratio," World Water & Environmental Resources Congress 2003: pp. 1-10. doi: 10.1061/40685(2003)308.

Yochum, S.E. (2012) "High Park Fire: Increased Flood Potential Analysis," USDA NRCS, Colorado State Office, doi:10.13140/2.1.1282.3047

Yochum, S.E., Norman, J. (2014) "West Fork Complex Fire: Potential Increase in Flooding and Erosion" USDA NRCS, Colorado State Office, doi:10.13140/2.1.4165.8887.